

TUBE WAVE ANALYSIS OF BURIED PIPES

N. M. Alam Chowdhury^{*1}, Z. Liao², L. Zhao¹ and C. T. Yang³

¹Dept of Electrical & Computer Engineering, Ryerson University, Canada

²Dept of Architectural Science, Ryerson University, Canada

³School of Information & Electronic Engineering, Zhejiang University of Science & Technology, China
e-mail: m9chowdh@ryerson.ca

ABSTRACT

Acoustic wave propagation of wire-break related events (WRE) in fluid-filled prestressed concrete cylinder pipes (PCCP) are of interest in non-destructive pipe detection. The mathematical model is developed based on Navier's equation of motion for the acoustic wave propagation. Newton's law of motion in equilibrium is used to model fluid-structure interaction. The analysis of acoustic pressure effect on pipe structure is developed by the principle of virtual work. To understand the characteristics of WRE vibration and the impact of path on the vibration signal, the dispersion behaviour of wave propagation is analyzed for various pipe profiles. It is observed that the speed of waves traveling in the fluid surrounded by the finite stiffness pipe profile is lower than the actual speed of acoustic waves of WRE signal in the unbounded fluid or fluid surrounded by infinite stiffness medium. Finite-element based software is used to simulate the results, which are compared with the available theoretical solutions.

RÉSUMÉ

La propagation d'onde acoustique de fil-cassent (wire break) les événements relatifs (WRE) dans des pipes remplies de fluide de cylindre de béton contraint d'avance (PCCP) sont d'intérêt pour la détection non destructive de pipe. Le modèle mathématique développé est basé sur l'équation du mouvement de Navier pour la propagation d'onde acoustique. La loi de Newton du mouvement dans l'équilibre est employée pour modéliser l'interaction de fluide-structure. L'analyse structurale de l'effet acoustique de pression sur la structure de pipe est expliquée par le principe du travail virtuel. Pour comprendre les caractéristiques de la vibration de WRE et l'impact du chemin sur la vibration signale, le comportement de dispersion de la propagation des ondes est analysé en utilisant divers profils de pipe. On l'observe que la vitesse des vagues voyageant dans le fluide entouré par le profil fini de pipe de rigidité est inférieure que la vitesse réelle des ondes acoustiques du signal de WRE en fluide illimité ou fluide entouré par milieu infini de rigidité. Le logiciel est employé pour simuler les resultants.

1. INTRODUCTION

The vibration signal generated by acoustic emission (AE) of WRE in PCCP is related to deterioration and passes through a number of media, such as pipes, water and surrounding media, before the signal is picked up by the sensors. This wave propagation can be modeled as the convolution of the WRE signal and the impulse response of the pipe. The impulse response of the pipe is dependent on water flow, diameter, thickness and stiffness of the pipe, and surrounding media. Since the PCCP has a cylindrical shape, the acoustic wave received by the hydrophone and/or accelerometer can be considered as the superposition of the different delayed version of WRE signal due to multipath propagation. Therefore, it is important to understand how the path physically affects the signal.

At low frequencies, where the wavelengths are much larger than the pipe radius, the Stoneley or tube mode is the only propagating mode with plane wavefronts in the fluid [1-8]. Hence, the plane wave propagation is used to measure the impact of path on the WRE signal. However at high frequencies, Rayleigh or shear modes exist which exhibit oscillatory amplitudes in the fluid and a decaying

amplitude in the pipe and surrounding medium. Therefore, care should be taken during the simulations to avoid excitation of higher-order modes for meaningful results.

Different methods [9-20] had been developed for the detection of wire failure and to locate the corroded areas. A large body of work exists that analyze the guided wave propagation through cylindrical pipe. These are mainly focused on guided wave (e.g. harmonic wave, axisymmetric and non-axisymmetric waves, multimode wave, lamb and love wave, ultrasonic wave, leaky wave, etc.) propagation through elastic, non-elastic, coated, non-coated, hollow and fluid-filled circular cylinder surrounded by fluids or solids [21-34].

This research goes beyond the previous works and emphasizes the effect of the path to appropriately model the impacts of the path on the spectral profiles of the vibration signals in different locations throughout the PCCP. An acoustical model is developed from Navier's equation of motion which can simulate vibrating WRE signal propagation through fluid-filled PCCP. The interaction of this propagation with the pipe structure is modeled by using Newton's law of motion in equilibrium. The principle of virtual work is used to develop the fluid-structure

interaction. The effect of the path is illustrated by tube wave analysis with different pipe profiles. The finite-element based commercial software is used to simulate the results which are then compared with the available theoretical results.

2. MODEL FORMULATION

The AE generated by wire break or slip (Fig.1) creates high frequency mechanical waves, which would immediately propagate along the pipe structure. This signal would also readily propagate into the pressurized fluid in the pipe at lower frequencies [35]. The PCCP structure mainly consists of concrete and steel components, which are highly attenuative compared to the fluid (water). For typical AE levels, the WRE signal that transmitted to the fluid column can be detected for several hundreds, perhaps thousands of feet [35]. On the contrary, in the pipe structure signals can travel only 100 to 200 feet for the same AE levels before they become strongly attenuated. However, for the sake of computational brevity, the analysis will be done assuming that the WRE signal starts to propagate from the fluid-pipe interface surface through fluid column only, which then interacts with the pipe wall. For the complete modeling of this propagation, applying the Navier's equation of motion is the most suitable approach.

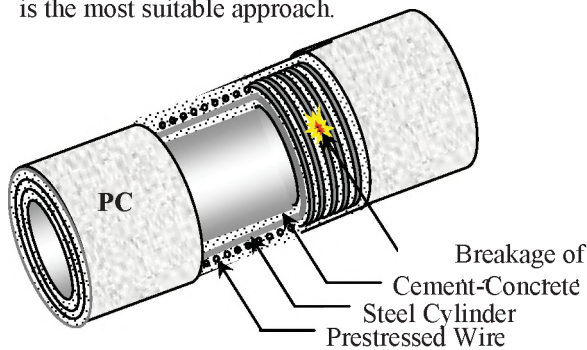


Figure 1. Illustrated view of PCCP construction and breakage of reinforced wire.

For a homogeneous isotropic elastic medium, the Navier's equation of motion is [36]

$$\mu \nabla^2 \mathbf{u} + (\lambda + \mu) \nabla (\nabla \cdot \mathbf{u}) = \rho \frac{\partial^2 \mathbf{u}}{\partial t^2}, \quad (1)$$

where \mathbf{u} is the time harmonic displacement field vector, μ and λ are the Lamé constants and ρ is the density of the medium.

The vector \mathbf{u} can be decomposed into scalar ϕ and vector $\boldsymbol{\psi}$ velocity potential as

$$\mathbf{u} = \nabla \phi + \nabla \times \boldsymbol{\psi}, \quad (2)$$

with the constraint [37]

$$\nabla \cdot \boldsymbol{\psi} = 0. \quad (3)$$

Substituting Eq.(2) into (1) and using vector identity yields

$$\nabla \left[(\lambda + 2\mu) \nabla^2 \phi - \rho \frac{\partial^2 \phi}{\partial t^2} \right] + \nabla \times \left[\mu \nabla^2 \boldsymbol{\psi} - \rho \frac{\partial^2 \boldsymbol{\psi}}{\partial t^2} \right] = 0. \quad (4)$$

The displacement Eq.(2) satisfies the equation of motion (4) if ϕ and $\boldsymbol{\psi}$ satisfy the following wave equations [38]

$$\nabla^2 \phi - \frac{1}{v_1^2} \frac{\partial^2 \phi}{\partial t^2} = 0, \quad (5)$$

$$\nabla^2 \boldsymbol{\psi} - \frac{1}{v_2^2} \frac{\partial^2 \boldsymbol{\psi}}{\partial t^2} = 0, \quad (6)$$

where

$$v_1 = \left[\frac{\lambda + 2\mu}{\rho} \right]^{1/2} \quad \text{and} \quad v_2 = \left[\frac{\mu}{\rho} \right]^{1/2}. \quad (7)$$

Eqs.(5) and (6) represents the longitudinal and shear wave equations where v_1 and v_2 represents the longitudinal and shear wave velocities of the medium, respectively.

2.1 Acoustic Pressure in the Fluid

The pressure (p) distribution of WRE signal for uniform flow in a lossless fluid can be expressed by using the pressure-velocity relation in Eq.(5) alone as

$$\frac{1}{\rho_F v_F^2} \frac{\partial^2 p}{\partial t^2} + \nabla \cdot \left(-\frac{1}{\rho_F} \nabla p \right) = 0, \quad (8)$$

where ρ_F is the fluid density and v_F is the speed of acoustic wave in the fluid medium.

The source that is of our interest in this model is the elastic energy that is stored in the prestressed wire of PCCP structure and released due to the breakage or slippage of the wire. The released energies appear as an AE of WRE signal [39]. The source of WRE signal on the fluid from the fluid-pipe interface is modelled as [40-42]

$$\mathbf{g} = \frac{\partial S}{\partial t} \delta^{(3)}(\mathbf{x} - \mathbf{x}'), \quad (9)$$

where S is the source flow strength that obtained from released elastic energy density, $\delta^{(3)}$ is the 3D Dirac delta function and \mathbf{x}' is the source location. Eq.(8) can be written as

$$\frac{1}{\rho_F v_F^2} \frac{\partial^2 p}{\partial t^2} + \nabla \cdot \left(-\frac{1}{\rho_F} \nabla p \right) = \mathbf{g}. \quad (10)$$

Eq.(10) represents the equation of WRE signal propagation through fluid-filled PCCP.

2.2 Fluid-Structure Interaction

The WRE signal that propagates through the fluid column appears as acoustic wave pressure on the pipe wall of the fluid-pipe interface and generates only small displacements. Since the pipe structure is much stiffer than the fluid, it will interact without causing separation or voids, which means that the radial displacements and pressure at the fluid-structure interfaces must be compatible and in equilibrium. Newton's law of motion in equilibrium is used to model this fluid-structure interaction.

2.2.1 Newton's Law of Motion in Equilibrium

The acoustic pressure force that acts on the pipe structure can be written as [42]

$$F_j = -n_j p, \quad (11)$$

where \mathbf{n} is the outward-pointing unit normal vector.

In equilibrium, the total work done in the pipe structure due to the displacements is equal to the work from external pressure forces. These forces undergo unrelated but consistent displacements and deformations, which can be expressed in terms of stresses as

$$F_j = -\frac{\partial \sigma_{ij}}{\partial x_i}, \quad (12)$$

where σ is the symmetric stress tensor consisting of normal and shear stresses and F is the body forces due to the external acoustic pressure acts in three principal directions. Eq.(12) represents the Newton's law of motion in equilibrium.

2.2.2 Principle of Virtual Work

The structural analysis of the fluid-structure interaction throughout the pipe structure can be explained by the Principle of Virtual Work (PVW). In this case, the virtual work on the pipe structure is the work resulting from acoustic wave's real pressure forces on the pipe, acting through a virtual displacement in terms of translation or rotation.

Let us consider an elastic and isotropic pipe structure with deformable body which consists of infinitesimal cubes as shown in Fig.2. Figure 2(a) shows external surface forces F^T , body forces F and internal stresses σ in equilibrium and Fig.2(b) shows continuous displacements \mathbf{u} and consistent strains ϵ .

The total virtual work (W_T) done by stresses or all forces, such as $F' = \sigma dydz$ (acts on individual common faces) and $F'' = \left(\sigma + \frac{\partial \sigma}{\partial x} dx \right) dydz$ (acts on other faces)

as shown in Fig.2(c), acting on the faces of all cubes which undergo unrelated but consistent [43] displacements and deformations can be written as [44]

$$W_T = -u_j F_j' + \left(u_j + \frac{\partial u_j}{\partial x_i} dx_i \right) F_j'' \quad (13)$$

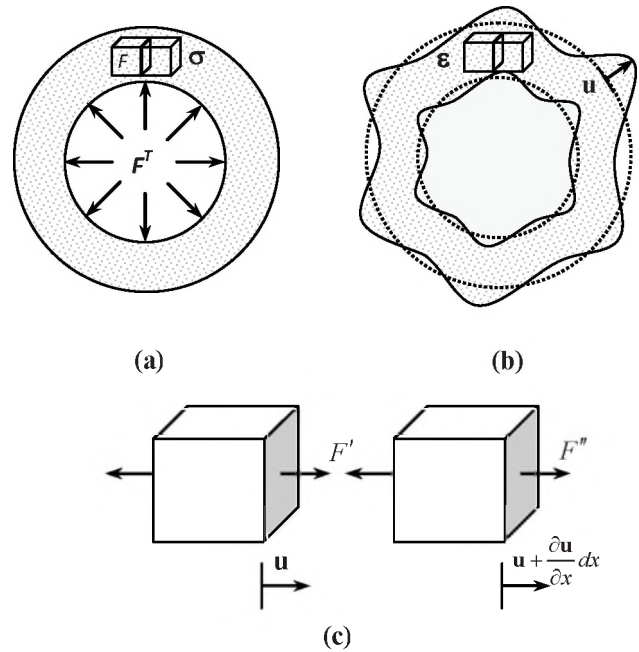


Figure 2. Virtual work on pipe structure, (a) Surface and body forces and stresses in equilibrium, (b) Consistent deformations and displacements, (c) Forces and displacements on cube faces.

By using Newton's second law of motion in equilibrium Eq.(12) and neglecting second order term, Eq.(13) can be written as

$$W_T \approx \frac{\partial u_i}{\partial x_j} \sigma_{ij} dv + u_j \frac{\partial \sigma_{ij}}{\partial x_i} dv = (\epsilon_{ij} \sigma_{ij} - u_j F_j) dv. \quad (14)$$

In Eq.(14), σ_{ij} and ϵ_{ij} are the normal and shear stress and strain distribution, respectively, within the deformed body, u_j and F_j are the displacements and body forces, respectively, acting in the three principal global directions. By taking the volume integral of Eq.(14) over the whole body, the PVW of surface and body forces can be expressed as

$$\int_s u_j F_j^T ds + \int_v u_j F_j dv = \int_v \epsilon_{ij} \sigma_{ij} dv. \quad (15)$$

In Eq.(15), the principle of virtual work states that the equilibrated stresses and body forces undergo unrelated but consistent displacements and strains only when internal virtual work is equal to the external virtual work. This satisfies the Newton's law of motion in equilibrium.

2.3 Displacement in the Structure

The Navier's equation of equilibrium in the pipe structure in terms of displacement vector \mathbf{u} can be obtained using stress-strain and strain-displacement relationships in Eq.(12). The stress-strain and strain-displacement relations for this model

can be expressed as

$$\sigma_{ij} = C_{ijpq} \varepsilon_{pq}, \quad (16)$$

and

$$\varepsilon_{ij} = \frac{1}{2} \left(\frac{\partial u_i}{\partial x_j} + \frac{\partial u_j}{\partial x_i} \right). \quad (17)$$

Here, C is the 6 x 6 elastic matrix which can be written as

$$C = \begin{bmatrix} (\lambda + 2\mu) & \lambda & \lambda & 0 & 0 & 0 \\ \lambda & (\lambda + 2\mu) & \lambda & 0 & 0 & 0 \\ \lambda & \lambda & (\lambda + 2\mu) & 0 & 0 & 0 \\ 0 & 0 & 0 & \mu & 0 & 0 \\ 0 & 0 & 0 & 0 & \mu & 0 \\ 0 & 0 & 0 & 0 & 0 & \mu \end{bmatrix}, \quad (18)$$

$$\Rightarrow C_{ijpq} = \delta_{ij} \delta_{pq} \lambda + (\delta_{ip} \delta_{jq} + \delta_{iq} \delta_{jp}) \mu, \quad (19)$$

where μ and λ are Lamé constants defined on the basis of elastic modulus E and Poisson's coefficient ν as

$$\mu = \frac{E}{2(1+\nu)}, \quad (20)$$

and

$$\lambda = \frac{\nu E}{(1+\nu)(1-2\nu)}. \quad (21)$$

For static case, using the above stress-strain relationship (Eq.16) and strain-displacement relationship (Eq.17) into Eq.(12), the displacement equation in the structure can be written as

$$\mathbf{F} = -\nabla \cdot (C \nabla \mathbf{u}). \quad (22)$$

In case of transient analysis, Eq.(22) can be expressed as [42]

$$\mathbf{F} = \rho \frac{\partial^2 \mathbf{u}}{\partial t^2} - \nabla \cdot (C \nabla \mathbf{u}). \quad (23)$$

Eq.(23) is used to calculate the displacement in the pipe structure due to acoustic pressure forces.

2.4 Tube Wave Analysis

The effect of path on low frequency WRE signal propagation can be illustrated by the tube wave analysis at different pipe profile. The characteristics of pipe profile mainly depend on dimensions and elastic properties of the pipe materials and the surrounding medium. The elastic waves that are generated in the pipe structure due to the AE signal depend on these characteristics. However, during the propagation this elastic wave is transmitted into the fluid and decreases the velocity of acoustic wave of WRE signal. This reduced wave is known as a 'Tube Wave.'

Mathematically, the expression for the tube wave (v_T) can be written as [45]

$$v_T = \left[\frac{1}{v_F^2} + \frac{\rho_F}{M_L} \right]^{-1/2}, \quad (24)$$

where

$$M_L = E_L \left[2(1+\nu_L) + \frac{D^2}{t(D+t)} \right]^{-1}, \quad (25)$$

and D is the diameter of the pipe, E_L , ν_L and t are the elastic (Young's) modulus, Poisson's ratio and thickness of the surrounding layered medium, respectively. The expression given in Eq.(24) is used to calculate the theoretical values of tube waves (v_T) of low frequency WRE signal, that propagate into the fluid-filled PCCP.

3. SOLUTION METHODOLOGY

In this paper, the numerical problem is solved for the pressure (p) distribution of WRE signals through the fluid-column only. During the solution, the fluid-structure coupling equations are used to simulate the effect of the surrounding medium into the acoustic pressure of the fluid. This section contains a general description of the numerical implementation steps, which are required for the simulation of any type of fluid-filled PCCP model.

3.1 Model Description

Consider a uniform and smooth circular pipe surrounded by soil formation and aligned along the x -direction. The base dimensions and the cross-sectional view of the model geometry are shown in Figure 3.

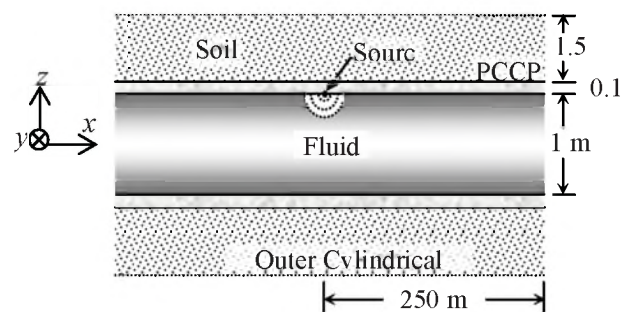


Figure 3. Cross-sectional view of model geometry.

For simplicity, consider a pipe structure of high-strength concrete only containing a stationary fluid medium. The simplification does not significantly impact the results of the analysis, but does result in a significant reduction in the computational resources [11]. Damping is absent in all media. The physical properties of the fluid (water) and surrounding solid materials are given in Table 1.

Table 1. Properties of the media.

| Properties | Fluid (Water) | Concrete | Soil |
|---|---------------|-----------------|------|
| Density of medium (ρ), kg/m ³ | 997 | 2400 | 1270 |
| Speed of acoustic wave (v), m/s | 1500 | -- | 463 |
| Elastic (Young's) modulus (E), Pa | -- | 40 ⁹ | -- |
| Poisson's ratio (ν) | -- | 0.33 | -- |

3.2 Boundary Conditions

The boundary conditions that are applied to this model are as follows:

- i. continuity of pressure in the fluid to pipe structure,
- ii. continuity of acceleration in the pipe to fluid/soil medium, and
- iii. radiation condition in the outer model boundary.

The acoustic pressure (in the fluid domain) of WRE signal acts as a boundary load on the 3D solid pipe structure to ensure continuity of pressure. Mathematically this boundary condition can be expressed as [42]

$$\mathbf{F} = -\mathbf{n}_F p, \quad (26)$$

where \mathbf{n}_F is the outward-pointing unit normal vector seen from inside the pipe structure.

This boundary load acts as an external force on the fluid-pipe surface which causes consistent displacements and deformations inside the pipe structure. According to the principle of virtual work, the total work from stress-strains of the structure is equal to the work from external forces. To satisfy the Newton's second law of motion, these stresses and strains are calculated using the normal acceleration of the pipe surface at the fluid boundary which ensures the continuity of acceleration.

The mathematical expression for the acceleration is

$$\mathbf{a}_n = -\mathbf{n}_a \cdot \nabla \mathbf{u}', \quad (27)$$

where \mathbf{n}_a represents the outward-pointing unit normal vector seen from inside the acoustic domain and (\cdot) represents the time derivative of displacement vector in three principal directions. Finally, the radiation boundary condition, i.e., no reflections from the boundary, is used on the outer perimeter of the model. Along the pipe axis, the radiation boundary condition is used with the plane wave propagation as [46],

$$\mathbf{n} \cdot \left(\frac{1}{\rho_F} \nabla p \right) + \frac{1}{\rho_F v_F} \frac{\partial p}{\partial t} = 0. \quad (28)$$

At the outer cylindrical surface, the radiation condition with the cylindrical wave propagation is used as [47],

$$\mathbf{n} \cdot \left(\frac{1}{\rho_F} \nabla p \right) + \frac{1}{\rho_F} \left(\frac{1}{v_F} \frac{\partial p}{\partial t} + \frac{1}{2r} p \right) = 0, \quad (29)$$

where r is the shortest distance between sources to the point of interest.

3.3 Model Discretization

For the numerical solution, it is necessary to discretize the model into small segments with a fixed wavelength that must be resolved. In addition, small features in the geometry and/or near the interface boundary or source vicinity model have high local pressure gradients that must be resolved appropriately to obtain a consistent global solution.

The finite element method (FEM) based analysis is used to handle this mathematical integrity and coupling equation between different physical layers. The FEM based simulation software COMSOL Multiphysics[®] is used to handle these complex issues. This software can handle the coupling effect of acoustic pressure from the fluid to the structure and the displacement from the structure to the fluid and the outer medium, efficiently. In this particular model, the second order polynomial basis functions are used to derive the discretized model. The maximum element size of 0.2λ (where wavelength $\lambda = v/f$) is used with the second-order element to satisfy the rule-of-thumb minimum of ten degrees of freedom per wavelength for a reliable solution [42].

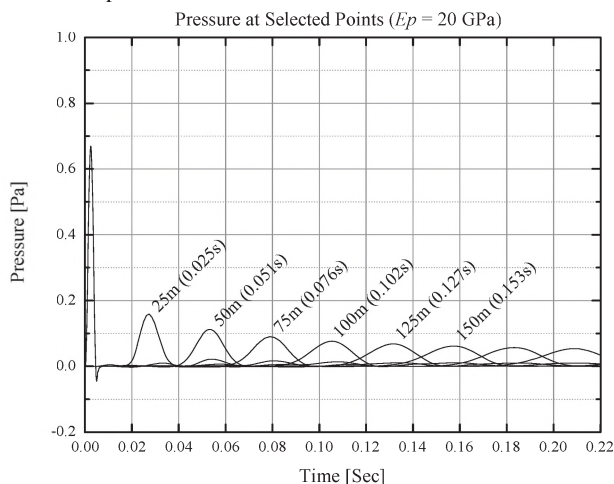
4 RESULTS AND DISCUSSION

The transient analysis of mathematical model outlined above is applied in two scenarios, namely water-filled pipe in air and in soil media. Commercial software COMSOL Multiphysics[®] is used to simulate the problem. During the simulation, different dimensions and stiffness of the layered media were investigated. This illustrates the effect of pipe profiling on tube mode propagation of WRE signal through water-filled PCCP. All simulations are done for the 0.2 kHz excitation frequency as this frequency is below the first cut-off frequency of the chosen pipe and the wavelength is greater than the diameter of the pipe for tube wave analysis [4]. The constant volume velocity source [48] is used with the source flow strength 1×10^{-2} m³/s, to optimize the result. In order to verify the simulation results with the calculated theoretical values from Eq.(24), the time response of the system is taken at selected points in the pipe - at 0m, 25m, 50m, 75m, 100m, 125m, 150m, 175m, 200m from source.

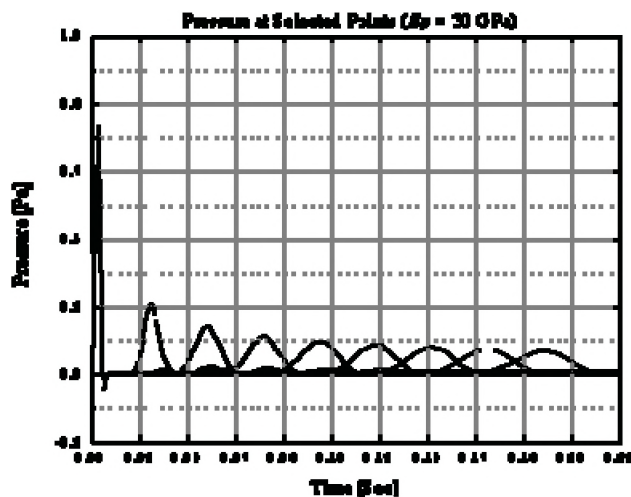
4.1 Effect of Pipe Elasticity

In this case we consider the water-filled pipe in air medium. The pipe with radius $R = 0.5$ m and thickness $t_p = 0.1$ m is used for this purpose. The elastic (Young's) modulus (E_p) of the pipe materials varies as 20GPa, 30GPa and 40GPa with densities (ρ_p), 2200 kg/m³, 2300 kg/m³ and 2400

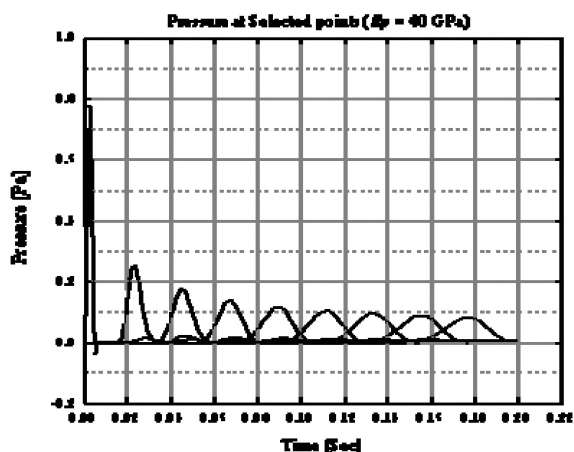
kg/m³, respectively. Other properties of the pipe and the fluid are kept constant as in Table-1.



(a) $E_p = 20\text{GPa}$ (calculated $V_T = 980\text{ m/s}$).



(b) $E_p = 30\text{GPa}$ (calculated $V_T = 1090\text{ m/s}$).



(c) $E_p = 40\text{GPa}$ (calculated $V_T = 1169\text{ m/s}$).

Figure 4. Tube wave response of water-filled PCCP (a) $E_p = 20\text{GPa}$, (b) $E_p = 30\text{GPa}$, and (c) $E_p = 40\text{GPa}$.

From Figure 4 it is seen that, the calculated theoretical tube wave velocities V_T , which is given below in each

graph, is matched with wave speed as seen in the simulation results. As for example in Fig.4(a), the calculated V_T is 0.98 km/s , therefore, the time required to travel the WRE signal from source to 50m distance is 0.051 sec , which is same as seen in the graph. Similarly, we can verify the simulation results for other distances.

From the results shown in Fig.4 we can also observed that, the propagation speed is reduced to a lower speed due to the tube wave effect [4], compared to the speed of the acoustic wave in the water (approximately 1500 m/s). The pipe stiffness increases with the increasing pipe elastic properties, which increases the wave's signal strength. This is the case because, the amount of signal energy penetration throughout the pipe structure decreases with the increasing pipe stiffness. Therefore, in all of the graphs above, it is clear that the WRE signal propagation in water-filled PCCP is affected significantly by the pipe properties.

4.2 Effect of Pipe Dimensions

To observe the effect of pipe dimensions, the variable dimensioned water-filled pipe in an air medium with fixed pipe properties ($E_p = 40\text{GPa}$, $\rho_p = 2400\text{ kg/m}^3$) is used.

In this case pipe thicknesses of $t_p = 0.1\text{m}$, 0.15m and 0.2m with a fixed pipe radius ($R = 0.5\text{m}$) is used. Next the pipe radius is varied as ($R = 0.5\text{m}$, 1.0m and 1.5m) with a fixed pipe thickness of $t_p = 0.1\text{m}$. The other properties of the pipe and the fluid medium are taken from Table 1. The results for the $R = 0.5\text{m}$ and $t_p = 0.1\text{m}$ pipe are same as the results shown in Figure 4(c) and for other dimensions results are shown in Figures 5 and 6, respectively.

It is seen from the Figures 5 and 6 that the simulation results of wave speed are in agreement with the theoretical calculated value given below in each graph. Moreover, from Figures 4(c) and 5, it is seen that increasing pipe thickness increases the stiffness, which increases tube wave speed. On the contrary from Figures 4(c) and 6, it can be seen that increasing the pipe radius decreases the system stiffness, resulting in a decreased tube wave speed. In both cases, signal strength decreases with the decreasing pipe stiffness. The important conclusion from this section is that WRE signal propagation in water-filled PCCP is affected by the pipe dimensions.

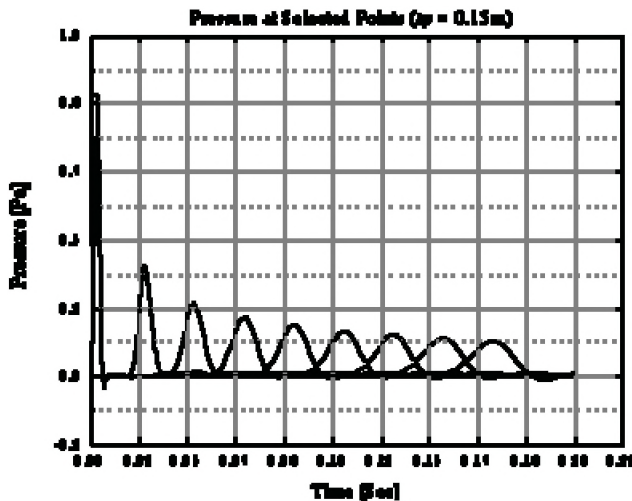
4.3 Effect of Soil Medium

Next, the effect of surrounding soil formation on water-filled pipes is explored. The thickness of the cylindrical soil layer (t_s) is taken as three time the pipe radius to optimize the results. All other variables, such as, pipe dimensions (e.g. $R = 0.5\text{m}$, $t_p = 0.1\text{m}$), pipe properties (e.g. $E_p = 40\text{GPa}$, $\rho_p = 2400\text{ kg/m}^3$), fluid properties (Table 1), etc. are kept as constants. Unlike the case of fluid or pipe material properties, the selection of soil properties cannot be known with same accuracy due to numerous uncertainties. The soil properties vary according to type and the depth of the pipe.

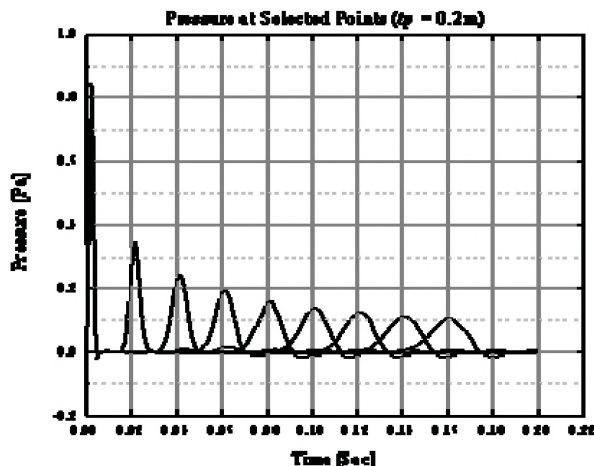
However, in this work the focus is the extent to which soil properties affect WRE signal propagation in water-filled PCCPs. Therefore, we choose three kinds of soil sample from the soil textural triangle [49], such as, Sandy Loam (Adrian soil), Silt Loam (Catlin soil) and Sand (Plainfield soil), to cover the wide range of soil elastic properties, shown in Table 2.

Table-2: Properties of the soil sample [50].

| Soil Sample | Soil Series (Code) | Density (ρ_s), kg/m ³ | Propagation Speed (v), m/s |
|-------------|--------------------|---|--------------------------------|
| Sandy Loam | Adrian (ADA) | 920 | 373 |
| Silt Loam | Catlin (CAB) | 1270 | 463 |
| Sand | Plainfield (PLA) | 1510 | 634 |



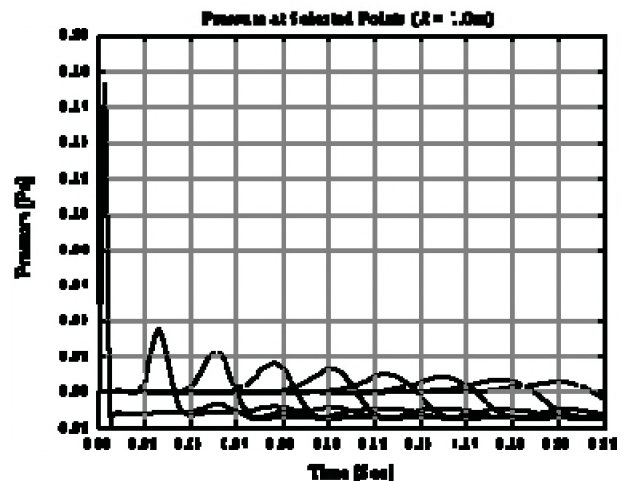
(a) $R = 0.5\text{m}$, $t_p = 0.15\text{m}$ (calculated $V_T = 1240\text{ m/s}$).



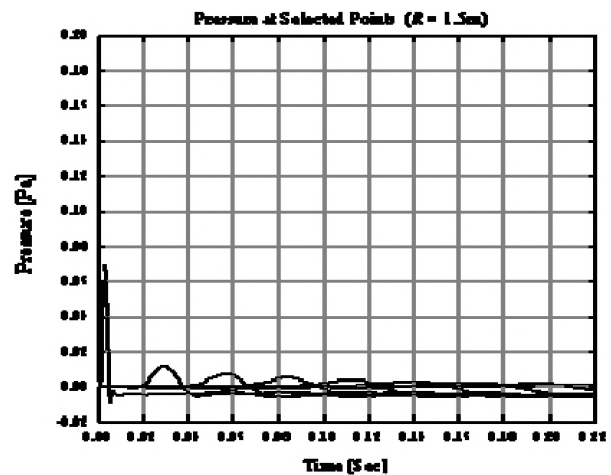
(b) $R = 0.5\text{m}$, $t_p = 0.2\text{m}$ (calculated $V_T = 1280\text{ m/s}$).

Figure 5. Tube wave response of water-filled PCCP

(a) $t_p = 0.15\text{m}$ and (b) $t_p = 0.2\text{m}$.



(a) $R = 1.0\text{m}$, $t_p = 0.1\text{m}$ (calculated $V_T = 1000\text{ m/s}$).



(b) $R = 1.5\text{m}$, $t_p = 0.1\text{m}$ (calculated $V_T = 900\text{ m/s}$).

Figure 6. Tube wave response of water-filled PCCP - (a) $R = 1.0\text{m}$ and (b) $R = 1.5\text{m}$.

Figures 7(a), (b), and (c) show the simulation results of WRE signal propagation through the pipe, which is surrounded by the Adrian, Catlin and Plainfield soil, respectively. By comparing these results with the theoretical tube wave velocities V_T , which is given below each graph, found a good agreement. However, if we compare these results with the result of same pipe in air medium (Fig.4c), we can see that the tube wave velocities are nearly the same in all cases. This means that, surrounding soil formation does not have any significant effect on tube wave propagation. This is believed to arise from the fact that the stiffness of the soil medium is only one thousandth of stiffness of the PCCP. Therefore, from the graphs above, it is clear that the WRE signal propagation in water-filled PCCP is not affected by the surrounding soil medium.

4.4 Effect of Guided Path

The other effects observed in the simulation results can be explained by the effect of guided path as follows. In the model a long circular shaped pipe is used, which acts as a

cylindrical wave guide for the WRE signal propagation. The excitation frequency is 200 Hz, which is below the first cut-off frequency of the pipe. Therefore, from the simulation results (Figs.4, 5, 6 and 7) it is observed that, there is only ‘zero’ order mode propagation exists in the pipe. During propagation, the initial pulse is extended due to the dispersion of the wave’s high frequency components. The signal level in the graphs decreases rapidly with the distance from the source. Initially, this signal travels at a very high speed, because close to its source, it travels as a spherical wave. Later on, when the wave extends over the entire cross-sectional area of the pipe, it travels as a planar wave with the expected speed of the main signal. Therefore, size and shape of the path also affects WRE signal propagation.

5 CONCLUSIONS

A mathematical model was developed to observe the WRE signal propagation through fluid-filled PCCP. The impact of the path on WRE signal propagation was illustrated by the tube wave analysis at different pipe properties. It was observed that the speed of the waves traveling in the fluid surrounded by the finite stiffness pipe was lower than the actual speed of the waves in an unbounded fluid. The tube wave effects were observed under plane-wave propagation and verified with the calculated theoretical values. From the simulation results, it was found that, the tube wave speed depends on pipe stiffness which mainly depends on elastic properties of the pipe materials as well as dimensions of the pipe. The stiffness of the pipe increased with increasing of the elastic properties of the pipe materials and the pipe thickness. On the contrary; it decreased with increasing pipe radius. It was also seen that the higher the stiffness, the higher the rigidity of the pipe, and lesser its influences on tube waves.

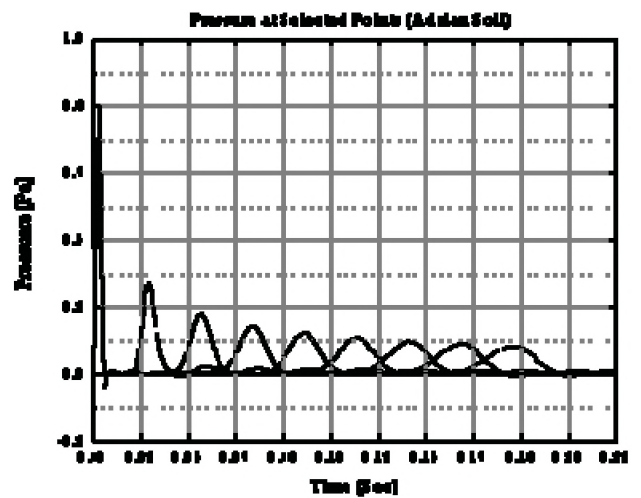
In contrast to the soil properties, the pipe profile, which depends on the pipe materials and dimensions, played an important role on the overall system stiffness. Therefore, in case of high stiffness pipe profile, there was no need to pay attention to the accurate estimation of soil parameters. Moreover, from the simulation results it was observed that the high stiffness pipe can reduce the signal energy penetration from inside to outside of the pipe. This was an important note for the WRE signal when it is measured by the sensor far away from the source.

6 ACKNOWLEDGEMENT

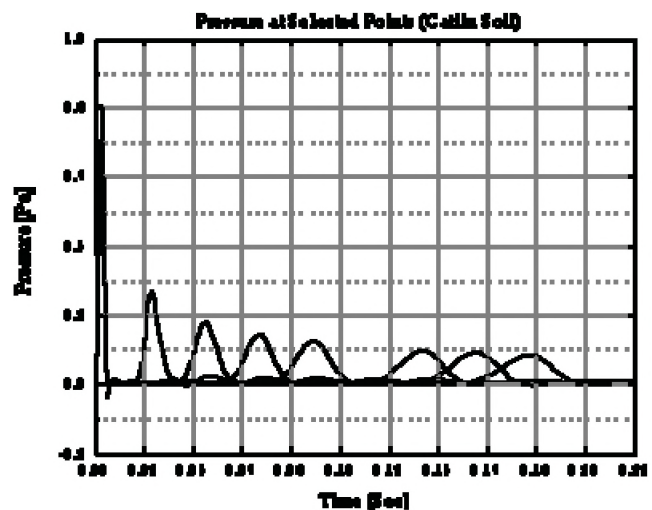
This work has been supported by the Ontario Centres of Excellence (OCE) under Grant No. EE50196.

7 REFERENCES

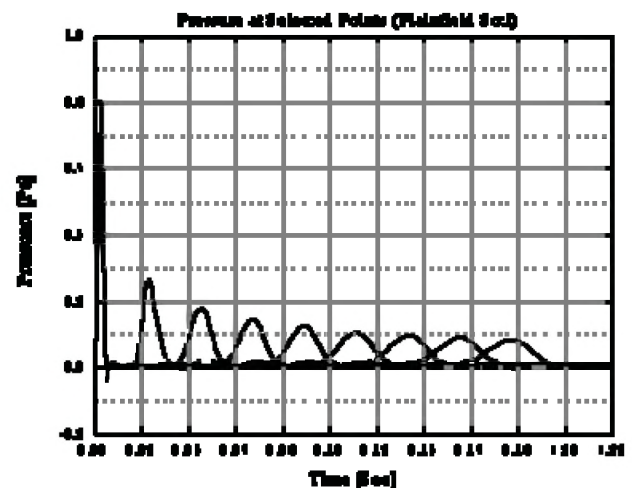
- [1] R.D. Fay, R.L. Brown and O.V. Fortier, “Measurement of acoustic impedances of surfaces in water,” *J. Acoust. Soc. Am.*, vol. 19, pp. 850-856, 1947.
- [2] W.L. Jacobi, “Propagation of sound waves along liquid cylinders,” *J. Acoust. Soc. Am.*, vol. 21, pp. 120-127, 1949.



(a) Adrian soil (calculated $V_T = 1169$ m/s).



(b) Catlin soil (calculated $V_T = 1170$ m/s).



(c) Plainfield soil (calculated $V_T = 1172$ m/s).

Figure 7. Tube wave response of water-filled PCCP (a) Adrian soil, (b) Catlin soil, and (c) Plainfield soil.

- [3] M.P. Home and R.J. Hansen, "Sound propagation in a pipe containing a liquid of comparable acoustic impedance," *J. Acoust. Soc. Am.*, vol. 71, pp. 1400-1405, 1982.
- [4] J.E. White, *Underground Sound: Application of Seismic Waves*, Elsevier Science, NY, 1983.
- [5] L.D. Lafleur and F.D. Shields, "Low-frequency propagation modes in a liquid-filled elastic tube waveguide," *J. Acoust. Soc. Am.*, vol. 97, no. 3, pp. 1435-1445, 1995.
- [6] V. Easwaran and M.L. Munjal, "A note on the effect of wall compliance on lowest-order mode propagation in fluid-filled/submerged impedance tubes," *J. Acoust. Soc. Am.*, vol. 97, no. 6, pp. 3494-3501, 1995.
- [7] J.E. Greenspon and E.G. Singer, "Propagation in fluids inside thick viscoelastic cylinders," *J. Acoust. Soc. Am.*, vol. 97, no. 6, pp. 3502-3509, 1995.
- [8] V.N.R. Rao and J.K. Vandiver, "Acoustics of fluid-filled boreholes with pipe: Guided propagation and radiation," *J. Acoust. Soc. Am.*, vol. 105, no. 6, pp. 3057-3066, 1999.
- [9] A.W. Peabody, "Control of pipeline corrosion", *National Assoc. of Corrosion Engineers*, Houston, 1967.
- [10] R.E. Price, and M.B. Brooks, "Evaluation of concrete pressure pipelines and prevention of failures," *Proc. Am. Soc. of Civil Engineers Annual Convention*, San Diego, CA, 1995.
- [11] F.A. Travers, "Acoustic monitoring of prestressed concrete pipe," *Constr. Building Mater.*, vol. 11, no. 3, pp. 175-187, 1997.
- [12] J. Makar, "Evaluation of acoustic monitoring for prestressed concrete cylinder pipe," *NRC Report B-5103.1*, National Research Council, Ottawa, ON, 1998.
- [13] D. O'Day, "External corrosion in distribution systems," *J. Am. Water Works Association*, Oct., pp. 45-52, 1969.
- [14] R. Wirahadikusumah, D.M. Abraham, T. Iseley, and R.K. Prasanth, "Assessment technologies for sewer system rehabilitation," *Automation in Constr.*, vol. 7, no. 4, pp. 259-270, 1998.
- [15] G. Phetteplace, "Infrared thermography for condition assessment of buried district heating piping," *Trans. ASHRAE*, vol. 105, part 2, pp. 776-781, 1999.
- [16] B. Mergelas, "Personal communication," Report : Pressure Pipe Inspection, Mississauga, ON, 1998.
- [17] D. Sack, and L. Olson, "In site nondestructive testing of buried precast concrete pipe," *Proc. Am. Soc. Civil Engineers*, Materials Engineering Conference, Sand Diego, Nov. 13-16, 1994.
- [18] N. Krstulovic Opara, R.D. Woods, N. Al Shaye, "Nondestructive testing of concrete structures using the rayleigh wave dispersion method," *J. Am. Concrete Institute Mater.*, vol. 93, no. 1, pp. 75-86, 1996.
- [19] J.M. Makar, and N. Chagnon, "Inspecting systems for leaks, pits, and corrosion," *J. Am. Water Works Association*, vol. 91, no. 7, pp. 36-46, 1999.
- [20] R. Bernstein, M. Oristaglio, D.E. Miller, and J. Haldorsen, "Imaging radar maps underground objects," *Computer Applications in Power*, vol. 13, no. 3, pp. 20-24, 2000.
- [21] D. C. Gazis, "Three-dimensional investigation of the propagation of waves in hollow circular cylinders: I - Analytical foundation," *J. Acoust. Soc. Am.*, vol. 31, no. 5, pp. 568-573, May 1959.
- [22] D. C. Gazis, "Three-dimensional investigation of the propagation of waves in hollow circular cylinders: II - Numerical results," *J. Acoust. Soc. Am.*, vol. 31, pp. 573-578, 1959.
- [23] H. J. Shin, *Non-Axisymmetric Ultrasonic Guided Waves For Tubing Inspection*, Ph.D. thesis, Pennsylvania State University, PA, USA, May 1997.
- [24] M. J. Quarry and J. L. Rose, "Multimode guided wave inspection of piping using comb transducers," *J. Mater. Eval.*, vol. 57, no. 10, pp. 1089-1090, 1999.
- [25] D. N. Alleyne and P. Cawley, "Long range propagation of lamb waves in chemical plant pipework," *J. Mater. Eval.*, vol. 45, no.4, pp. 504-508, 1997.
- [26] D.E. Chimenti, A.H. Nayfeh, and D.L. Butler, "Leaky waves on a layered half-space," *J. Appl. Phys.*, vol. 53, pp. 170-176, 1982.
- [27] J. Ditri, J.L. Rose, and G. Chen, "Mode selection guidelines for defect detection optimization using lamb waves," *Proc., 18th Annual Review of Progress in Quantitative NDE Meeting, Plenum*, vol. 11, pp. 2109-2115, Brunswick, ME, 1991.
- [28] R.M. Cooper, and P.M. Naghdi, "Propagation of nonaxially symmetric waves in elastic cylindrical shells," *J. Acoust. Soc. Am.*, vol. 29, pp.1365-1373, 1957.
- [29] A.H. Fitch, "Observation of elastic pulse propagation in axially symmetric and nonaxially symmetric longitudinal modes of hollow cylinders," *J. Acoust. Soc. Am.*, vol. 35, pp. 706-707, 1963.
- [30] J.N. Barshinger, J.L. Rose, "Ultrasonic guided wave propagation in pipes with viscoelastic coatings," *QNDE*, Brunswick, ME, July 29-August 3, 2001.
- [31] Y. Cho, and J.L. Rose, "Guided waves in a water loaded hollow cylinder," *J. Nondestructive Testing and Eval.*, vol. 12, pp. 323-339, 1996.
- [32] Y.H. Pao, and R.D. Mindlin, "Dispersion of flexural waves in an elastic circular cylinder," *ASME J. Appl. Mech.*, vol. 27, pp. 513-520, 1960
- [33] I.A. Viktorov, "Rayleigh-type waves on a cylindrical surface," *Soviet Phys. Acoust.*, vol. 4, pp. 131-136, 1958.
- [34] J.Jr. Zemanek, "An experimental and theoretical investigation of elastic wave propagation in a cylinder," *J. Acoust. Soc. Am.*, vol. 51, pp. 265-283, 1972.

- [35] F.B. Stulen and J.F. Kiefner, "Evaluation of acoustic emission monitoring of buried pipelines," *Proc. IEEE Ultra. Symp.*, pp. 898-903, 1982.
- [36] J. N. Barshinger and J. L. Rose, "Guided wave propagation in an elastic hollow cylinder coated with a viscoelastic material," *IEEE Trans. Ultrason., Ferroelect., Freq. Contr.*, vol. 51, no. 11, pp. 1547-1556, Nov. 2004.
- [37] K.F. Graff, *Wave Motion in Elastic Solids*, NY: Dover, 1991.
- [38] J.D. Achenbach, *Wave Propagation in Elastic Materials*, NHPC, 1973.
- [39] O. Tozser and J. Elliott, "Continuous acoustic monitoring of prestressed structures," in *Proc. CSCE Struct. Specialty Conf.*, 2000.
- [40] P.A. Martin and J.R. Berger, "On mechanical waves along aluminum conductor steel reinforced (ACSR) power lines," *ASME J. Appl. Mech.*, vol. 69, no. 6, pp. 740-48, 2002.
- [41] Y.Z. Pappas, A. Kotsos, T.H. Loutas and V. Kostopoulos, "On the characterization of continuous fibres fracture by quantifying acoustic emission and acousto-ultrasonics waveforms," *Elsevier: NDT & E. Int.*, vol. 37, no. 5, pp. 389-401, 2004.
- [42] COMSOL 3.4: *Acoustics Module - User's Guide*, Comsol User Doc., COMSOL AB, Stockholm, 2007.
- [43] B. Torby, *Energy Methods*, Advanced Dynamics for Engineers, HRW Series in Mechanical Engineering, CBS College Publishing, USA, 1984.
- [44] C. Jong, "Teaching students work and virtual work method in statics: A guiding strategy with illustrative examples," *Proc. American Soc. for Engineering Education Annual Conf. & Exposition*, ASEE, 2005.
- [45] P.M. Morse and H. Feshbach, *Methods of Theoretical Physics-II*, McGraw-Hill, NY, 1953.
- [46] D. Givoli and B. Neta, "High-order non-reflecting boundary scheme for time-dependent waves," *J. Comput. Phys.*, vol. 186, pp. 24-46, 2004.
- [47] A. Bayliss, M. Gunzburger and E. Turkel, "Boundary conditions for the numerical solution of elliptic equations in exterior regions," *SIAM J. App. Math.*, vol. 42, no. 2, pp. 430-451, 1982.
- [48] H. Y. Lee, *Drillstring Axial Vibration and Wave Propagation in Boreholes*, Ph.D. thesis, MIT, Cambridge, MA, USA, May 1991.
- [49] F. Adamo, G. Andria, F. Attivissimo and N. Giaquinto, "An acoustic method for soil moisture measurement," *IEEE Trans. Instrum. Meas.*, vol. 53, no. 4, pp. 891-898, Aug. 2004.
- [50] M.L. Oelze, W.D. O'Brien and R.G. Darmody, "Measurement of attenuation and speed of sound in soils," *J. Soil Sci. Soc. Am.*, vol. 66, pp. 788-796, 2002.



Freedom Step

Convert a standard floor to a superior floor with the Freedom Step Acoustical & Impact Isolation Subfloor

AcustiFloat®
Acoustical & Impact Subfloor Systems

WILREP LTD.

Tel. (905) 625-8944 Toll Free 1-888-625-8944

www.acoustifloat.com

Gym Rooms Playrooms Home Theaters Dance Floors

AcustiFloat is a registered Trademark of WILREP LTD.

In a Class of its Own

The unmistakable look of Hand-held Analyzer Type 2270 can overshadow a number of discrete yet significant distinctions which make this powerful instrument the complete toolbox for sound and vibration professionals. These include:

- Integrated digital camera
- Two-channel measurement capability
- Integrated LAN and USB interfaces for fast data transfer to PC and remote control and monitoring of Type 2270
- Environmental protection IP 44

Versatile in the Extreme

Type 2270 also boasts a wide range of application software modules that can be licensed separately so you get what you need when you need it.

Currently available measurement software includes:

- Sound Level Meter application
- Real-time frequency analysis
- Logging (noise level profiling)
- Sound and vibration recording
- Building acoustics
- Tonal assessment

Type 2270 meets the demands of today's wide-ranging sound and vibration measurement tasks with the accuracy and reliability associated with Brüel & Kjær instrumentation.

To experience the ease-of-use of Type 2270, just go to www.bksv.com and view the on-line video demonstrations.

For more information please contact your local Brüel & Kjær representative



HEADQUARTERS: DK-2850 Nærum · Denmark · Telephone: +4545800500
Fax: +4545801405 · www.bksv.com · info@bksv.com

Australia (+61)29889-8888 · Austria (+43)18657400 · Brazil (+55)115188-8166
Canada (+1)514695-8225 · China (+86)1068029906 · Czech Republic (+420)267021100
Finland (+358)9-755950 · France (+33)169907100 · Germany(+49)42117870
Hong Kong (+852)25487486 · Hungary (+36)12158305 · Ireland (+353)18037600
Italy (+39)025768061 · Japan (+81)337798671 · Republic of Korea (+82)234730605
Netherlands (+31)318 55 9290 · Norway (+47)66771155 · Poland (+48)228167556
Portugal (+351)214711453 · Singapore (+65)3774512 · Slovak Republic (+421)254430701
Spain (+34)916590820 · Sweden (+46)84498600 · Switzerland (+41)18807035
Taiwan (+886)227139303 · United Kingdom (+44)1438739000 · USA (+1)8003322040

Local representatives and service organisations worldwide

Hand-held Analyzer *Type 2270*

Brüel & Kjær 

Better testing... better products.

The Blachford Acoustics Laboratory

Bringing you superior acoustical products from the most advanced testing facilities available.



Our newest resource offers an unprecedented means of better understanding acoustical make-up and the impact of noise sources. The result? Better differentiation and value-added products for our customers.



Blachford Acoustics Laboratory features

- Hemi-anechoic room and dynamometer for testing heavy trucks and large vehicles or machines.
- Reverberation room for the testing of acoustical materials and components in one place.
- Jury room for sound quality development.



Blachford acoustical products

- Design and production of simple and complex laminates in various shapes, thicknesses and weights.
- Provide customers with everything from custom-engineered rolls and diecuts to molded and cast-in-place materials.

Blachford **QS 9000**
REGISTERED

www.blachford.com | Ontario 905.823.3200 | Illinois 630.231.8300

